The following publication Y. Tan, W. Jin, F. Yang, Y. Jiang and H. L. Ho, "Cavity-Enhanced Photothermal Gas Detection With a Hollow Fiber Fabry-Perot Absorption Cell," in Journal of Lightwave Technology, vol. 37, no. 17, pp. 4222-4228, 1 Sept., 2019 is available at https://doi.org/10.1109/JLT.2019.2922001.

Cavity-enhanced photothermal gas detection with a hollow fiber Fabry-Perot absorption cell

Yanzhen Tan, Wei Jin, *Senior Member*, *IEEE*, Fan Yang, Yi Jiang, and Hoi Lut Ho

***Abstract*—A photothermal (PT) gas sensor with a hollow-core photonic bandgap fiber (HC-PBF) Fabry-Perot absorption cell is demonstrated. The formation of a high finesse cavity enhances the pump intensity and hence PT phase modulation as well as the sensitivity of PT phase detection by a factor that is proportional to the cavity finesse. Experiments with a 6.2-cm-long HC-PBF absorption cell with a finesse of 45 for the pump and 41 for the probe achieved detection limit of 126 parts-per-billion (ppb) acetylene. The double-cavity-enhanced PT gas sensor allows the use of a shorter HC-PBF to develop highly sensitive and fast all-fiber gas sensors.**

***Index Terms*—Gas sensor, photonic crystal fiber, cavity enhancement, photothermal interferometry, optical fiber sensor.**

I. Introduction

Photothermal interferometry (PTI) is a highly sensitive gas detection technique. It detects the optical phase modulation of a probe beam resulting from the absorption of periodically modulated pump beam by the gas molecules. This technique has been used to detect gases including methanol [1], ammonia [2], and nitrogen dioxide [3].

The magnitude of photothermal (PT) phase modulation is proportional to gas absorption, optical path-length and intensity (instead of power) of the pump beam [4]. Conventional PTI systems uses open-path absorption cells, and the relatively large diameter of the free-space beams means large pump power is required to achieve sufficient pump intensity to generate detectable PT phase modulation [1]. Moreover, open-path sensors have limitations in realizing long absorption path due to loss and size problems. Long absorption path length can be achieved with multi-pass White cells [5] and Herriott cells [6], which are bulky, expensive and not convenient for field applications.

Recently, PT phase modulation in a gas-filled hollow-core photonic bandgap fiber (HC-PBF) was studied, and gas detection down to part-per-billion (ppb) level has been experimentally demonstrated with fiber-optic PTI [7]. In a HC-PBF, most of its optical power is confined in the hollow-core, and the mode field diameter of its fundamental mode is two orders of magnitude smaller than a typical open-path free-space beam. For the same level of pump power, the pump intensity in the hollow-core is much higher than in a free-space beam, enhancing significantly the PT phase modulation. The use of a HC-PBF also allows efficient gas-light interaction over a longer distance while maintaining compact size [8, 9]. With 10-m-long HC-PBF, detection of acetylene down to 2 ppb has been demonstrated [7]. However, the response time of the HC-PBF sensor is extremely long due to time taken for gas to diffuse into the hollow-core [10]. The speed of response may be improved by introducing side channels along the HC-PBF to accelerate gas diffusion [11-13]. However, it is challenging to achieve long-absorption-path (for better sensitivity) and fast response at the same time since it requires a huge number of side-channels.

The use of a HC-PBF Fabry-Perot (F-P) cavity as the absorption cell may overcome the predicament. A long effective path-length can be achieved with a high finesse cavity made with a short HC-PBF. We have previously reported a direct absorption spectroscopic gas sensor with a HC-PBF F-P cavity with finesse of 68 and achieved detection limit of 7 part-per-million (ppm) acetylene [14]. The sensitivity of the direct absorption HC-PBF sensor is limited by mode interference and other noises, and further improvement in the detection limit seems difficult [9, 14].

In this paper, we present a novel cavity-enhanced PT gas sensor with a high finesse HC-PBF F-P absorption cell. Comparing with a single path absorption cell, the intra-cavity pump intensity can be much higher and hence the magnitude of PT phase modulation can be enhanced significantly. In the meanwhile, the sensitivity of phase detection can also be enhanced by operating the probe at the highest slope point near a cavity resonance, resulting from the effective multi-passages of the probe beam through the gas sample. The enhancement factors for both PT phase modulation and detection are proportional to cavity finesses. This double enhancement allows the realization of high sensitivity with a short length of

Manuscript received XXX XXX; revised XXXX. This work was supported by the Hong Kong SAR government through GRF grant PolyU 152229/15E, Natural Science Foundation of China through NSFC grants 61535004 and 61827820, and the Hong Kong Polytechnic University through grants 1-ZVG4, and 4-BCD1 and 1-YW1R. (*Corresponding author: Wei Jin.*)

Y. Tan is currently with the School of of Electrical Engineering and Intelligentization, Dongguan University of Technology, Dongguan 523808, China and was with the Department of Electrical Engineering, The Hong Kong Polytechnic University, Hung Hom, Kowloon, Hong Kong (e-mail: yanzhentan@126.com).

W. Jin, F. Yang, and H. L. Ho are with the Department of Electrical Engineering, The Hong Kong Polytechnic University, Hung Hom, Kowloon, Hong Kong, and The Hong Kong Polytechnic University Shenzhen Research Institute, Nanshan District, Shenzhen, China. (e-mail: wei.jin@polyu.edu.hk; ee.yangfan@connect.polyu.hk; eehlho@polyu.edu.hk).

Y. Jiang is with the School of Opto-Electronics, Beijing Institute of Technology, Beijing, China. (e-mail: bitjy@bit.edu.cn).

HC-PBF, avoid the problem of slow response of a long HC-PBF gas cell.

II. Principles of Cavity-Enhanced PTI

The basic concept of cavity-enhanced PTI may be explained with the aid of Fig. 1. A high finesse HC-PBF cavity formed by placing a piece of HC-PBF between two reflective mirrors is filled with an absorptive gas. When the wavelength of a pump beam is tuned to one of the F-P cavity resonances (Resonance A), it is coupled into the cavity efficiently and the pump intensity inside the cavity is significantly higher than the input pump. Modulating the pump wavelength around the resonance results in modulation of the pump intensity in the cavity, with the magnitude of modulation proportional to the cavity finesse. If the cavity resonance lies within an absorption line of the absorptive gas, the absorption of the modulated pump will result in periodic heating, modulating the refractive index (RI) of the gas in the hollow-core and the dimensions of the HC-PBF [7]. When another probe beam is propagating in the same HC-PBF, its phase will be modulated accordingly, which can be detected by operating the probe at a maximum slope point of a different resonance (Resonance B) where the gas absorption is minimal. The sensitivity of phase detection, defined as the phase to intensity conversation efficiency at the probe wavelength, is proportional to the finesse of Resonance B. Hence, the use of a high finesse F-P gas cell provides double-enhancement, which enhances the PT phase modulation as well as the sensitivity of phase detection.

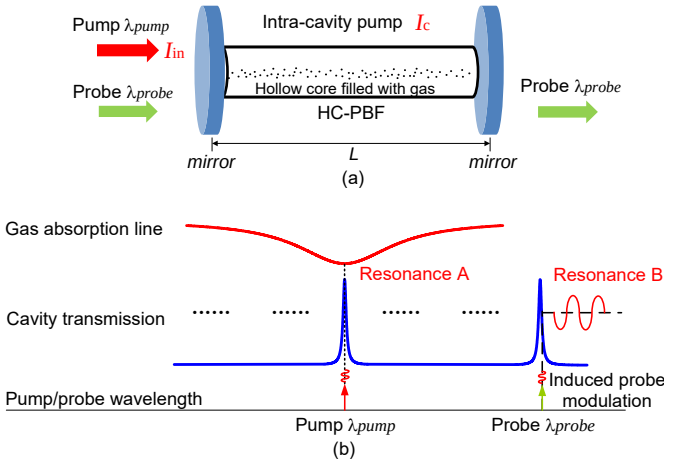

Fig. 1. Principles of cavity-enhanced PTI spectroscopy. (a) Sketch of a gas-filled HC-PBF F-P cavity. (b) Basic processes in the generation and detection of PT phase modulation.

A. Intra-cavity pump intensity

We first consider an empty F-P cavity with the length of L. The transmission and reflection coefficients, and the loss of the mirrors are respectively t, r and l, with $t+r+l=1$. The cavity finesse F and the on-resonance cavity transmission T_{res} may be expressed as [15-17]

$$F = \frac{\pi}{t+l} = \frac{\pi}{1-r} \tag{1}$$

$$T_{res} = \frac{t^2}{(1-r)^2} \tag{2}$$

The enhancement factor E, which is defined as the intra-cavity pump intensity I_c (or power P_c) over the input pump intensity I_{in} (or power P_{in}) may be expressed as [15-17]

$$E = \frac{I_c}{I_{in}} = \frac{P_c}{P_{in}} = t(\frac{F}{\pi})^2 \tag{3}$$

Comparing with a single-path gas cell of length L, the Fabry-Perot gas cell with finesse F enhances the pump intensity in the gas cell by a factor of E. Take a cavity with finesse of 1000 as an example and assume that the on-resonance cavity transmission T_{res} is 0.99, the enhancement factor E would be 300. For an input power of 1 mW, the intra-cavity pump power would be 300 mW, a huge enhancement over the input pump power.

B. Enhancement of PT phase modulation

Now the HC-PBF F-P cavity is filled with a weak absorptive gas with absorption coefficient α and concentration C. If the pump wavelength is modulated sinusoidally and its nominal wavelength is tuned to a cavity resonance aligned to the center of an absorption line (resonance A in Fig.1b), the magnitude of PT phase modulation through the gas-filled cavity may be expressed as [7,18]

$$\Delta\varphi = \Delta\bar{\varphi}_0 \cdot \alpha CL \cdot P_c \tag{4}$$

$\Delta\bar{\varphi}_0$ is a normalized phase modulation coefficient. For the NKT's HC-1550-02 fiber filled with trace acetylene balanced with nitrogen and with pump modulation frequency below 330 kHz, $\Delta\bar{\varphi}_0$ was determined to be $0.76 rad \cdot cm \cdot mW^{-1} \cdot m^{-1}$ [18-20]. The use of a resonating cell enhances the value of P_c (compared with P_{in}) and hence the PT phase modulation by a factor of E.

C. Enhancement of phase detection

The PT phase modulation can be detected by using the same F-P cavity by operating the probe wavelength at the highest slope point of Resonance B, as shown in Fig. 1(b). The F-P cavity converts the PT phase modulation into intensity (power) modulation at its output, which is proportional to the slope (1st-order derivative) of the cavity resonance. Figs. 2(a) and 2(b) illustrate respectively the normalized transmission and its 1st-order derivative of the cavity resonance with two different values of finesse. Obviously, the phase detection sensitivity varies with operating points. For the cavity resonance with F=50, the sensitivity (i.e., slope) is the highest at point 5 at which the probe beam should operate. For the cavity with F=2, the optimal operating point should be Point 6, but the slope, which is proportional F, is much smaller.

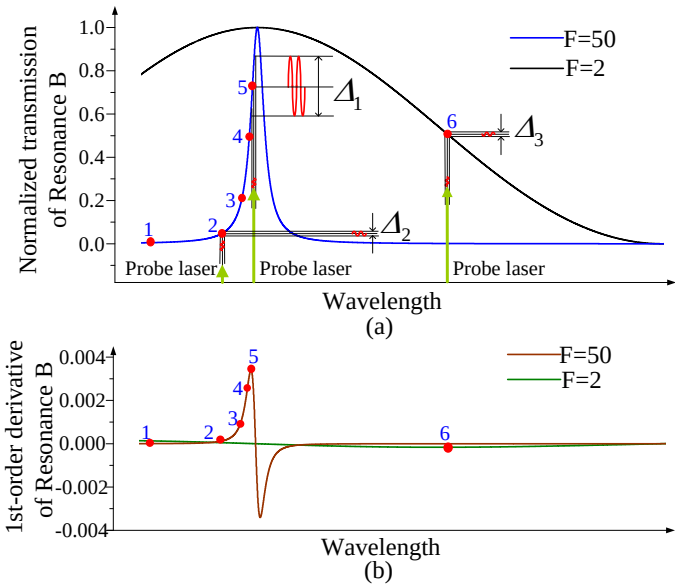

Fig. 2. Calculated (a) transmission and (b) 1st-order derivative of the cavity resonance with finesse of F=50 and F=2, respectively.

III. The HC-PBF F-P Gas Cell

The HC-PBF F-P absorption cell used in our work is illustrated in Fig. 3(a). The HC-PBF is the HC-1550-06 fiber with a core diameter of ~11 μm, as shown in Fig. 3(b). The length of the HC-PBF is 6.2 cm. The ends of the SMFs are coated with alternating dielectric layers (SiO_2 and TiO_2) to achieve reflectivity of ~99%. The SMFs ends were directly joined to the HC-PBF by mechanical splicing, without using any mode-matching lenses. The loss of a mechanical splice is ~4 to 6 dB, which is larger than the fusion splicing loss of ~2 dB [21].The fabrication process of the HC-PBF F-P gas cell was described in detail in Ref [14]. A small gap (<1 μm) was maintained at the SMF/HC-PBF joints for gas filling to the hollow-core.

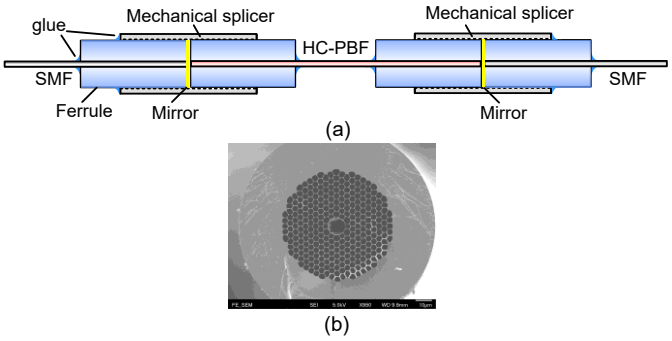

Fig. 3. (a) Schematic configuration of the HC-PBF F-P F-P gas cell. (b) Scanning electron micrograph of the HC-1550-06 fiber.

The finesse is defined as $F=FSR/\delta v$, where FSR and δv are respectively the free spectral range and full-width half-maximum spectral width (FWHM) of the cavity resonance [22]. For a cavity with length 6.2 cm, the FSR is calculated to be 18.9 pm at 1532 nm and 19.4 pm at 1550 nm. The transmission characteristics of the cavity at different wavelengths were recorded by sweeping the cavity with a multilayer piezo-ceramic stack (PZT) attached to the HC-PBF, as described in Ref [14]. Fig. 4(a) shows the sweeping voltage used to the PZT, while Figs. 4(b) and 4(c) show the measured transmissions of the cavity at two different laser wavelengths. The oscilloscope traces in Figs. 4(a), 4(b) and 4(c) are measured as functions time and the finesse can be determined by comparing the width of the resonators and spacing between the two resonances. In Fig. 4 (b), the laser wavelength is set to 1532.83 nm, the finesse of the cavity is determined to be 45. Similarly, in Fig. 4 (c), the wavelength is 1550.02 nm and the finesse is 41. These two wavelengths are used as the pump and probe wavelengths in the PT gas experiments in Section IV.

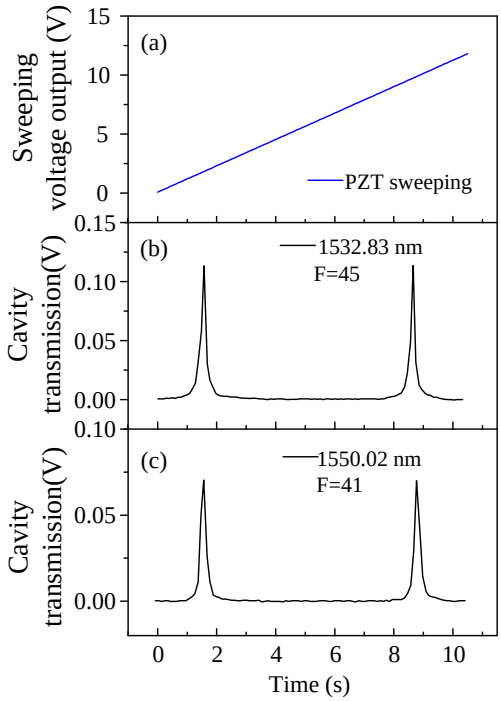

Fig. 4. (a) Sweeping voltage applied to PZT. Measured transmissions of the 6.2-cm-long HC-PBF F-P cavity at the wavelength of (b) 1532.83 nm and (c) 1550.02 nm.

IV. Cavity-Enhanced PT Gas Detection Experiments

A. Experimental setup

The cavity-enhanced PT gas experiments were conducted with the experimental setup in Fig. 5 (a). The cavity length of the gas cell is 6.2 cm and the FSR is ~19 pm (2.43 GHz), as described in Section III. The P(13) line of acetylene gas with center wavelength 1532.83 nm is used, and the linewidth of this line is ~40 pm or 5.11 GHz, which covers approximately 2.1 FSR of the F-P cavity, as indicated in Fig. 5 (b).

A distributed feedback (DFB) semiconductor laser is used as the pump beam and its wavelength (λ_{pump}) is slowly scanned across the P(13) line and the corresponding cavity resonances. The laser nominal wavelength is thermally tuned at a lower frequency of 0.001 Hz via a temperature controller and simultaneously modulated at a higher frequency of 22.4 kHz via current modulation. Fig. 5(b) illustrates the pump tuning process as well as the absorption line and the cavity resonances involved in the process. Ideally, cavity resonance A is at the

center of the absorption line, and pump beam tuned to this resonance is most efficiently coupled into the cavity and at the same time maximally absorbed by the gas molecules. Modulation of the pump wavelength causes periodically variation of the pump intensity in the cavity, resulting in phase modulation of the probe beam.

The probe beam is from an external cavity diode laser (ECDL) and the output power is ~3 mW. The probe laser wavelength (λ_{probe}) is tuned to 1550.2 nm, corresponding to highest slope point of Resonance B in Fig. 5 (b), which produces the largest intensity modulation in the output for a given PT phase modulation. The probe light from the cavity was received by a photo-detector (PD). The PD output was detected by a lock-in amplifier (Stanford research systems, SR830), and the second harmonic signal (i.e., 44.8 kHz) is used as the system output. The pump power at the output of 90:10 coupler in Fig. 5 (a) is measured to be 116.7 mW, and the pump power into the cavity is estimated to be~ 45 mW since the loss for the first mechanical splicing joint is ~4 dB. The acetylene concentration in the gas cell is 100 parts-per-million (ppm). The lock-in time constant is set to 3 s and the filter slope is 18 dB Oct^{-1}, corresponding to an effective detection bandwidth of 0.031 Hz. During this process, the probe laser wavelength is maintained at the highest slope point by monitoring the DC component of the transmitted F-P output and tuning the wavelength of the probe.

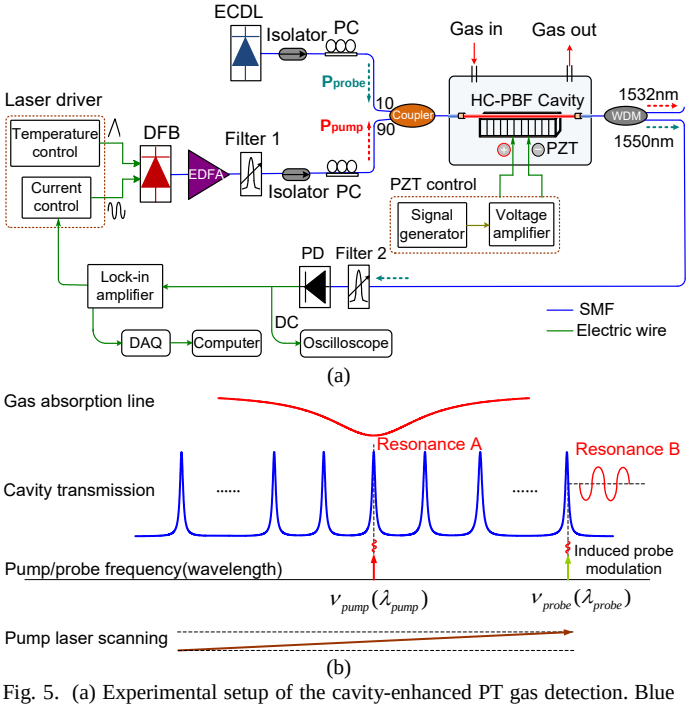

Fig. 5. (a) Experimental setup of the cavity-enhanced PT gas detection. Blue line, optical fiber; green line, electric cable; ECDL, external cavity diode laser; DFB, distributed feedback laser; PZT, piezoelectric stack; WDM, wavelength division multiplexer; PC, polarization controller; PD, photo-detector; DAQ, data acquisition. (b) Basic processes involved in the cavity-enhanced PT gas experiment.

B. *Experimental results*

Fig 6 shows the second harmonic signal from the lock-in when the wavelength of the pump was scanned across the P(13) line of acetylene and the corresponding cavity resonances. Fig. 6(a) shows second harmonic signal for the gas cell containing 100 ppm acetylene balanced with nitrogen. The blue line indicates the second harmonic signal which becomes maximal near the gas absorption line center at 1532.83 nm and gradually reduces away from the gas absorption line. The red line shows the theoretical P(13) absorption lineshape of acetylene obtained from HITRAN 2004 database [23]. Fig. 6(b) shows second harmonic output when the gas cell is filled with nitrogen. A small background thermal signal exists, which is believed due to the absorption of the dielectric mirrors [24].

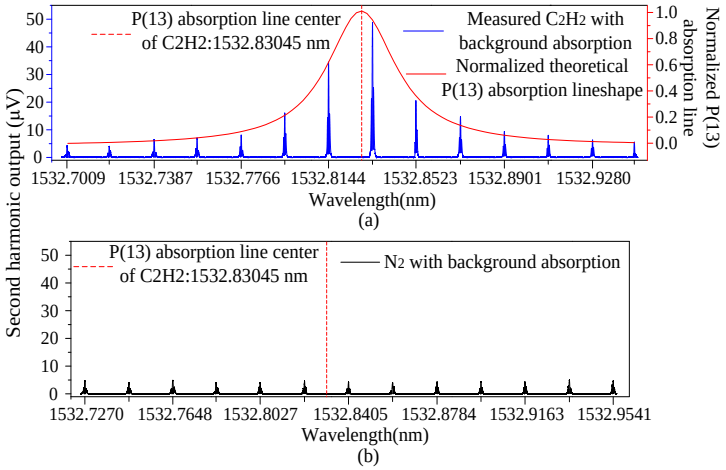

Fig. 6. Second harmonic output signal when pump laser is scanned across the P(13) line of acetylene and the corresponding cavity resonances. The gas cell is filled with (a) 100 ppm acetylene with nitrogen and (b) pure nitrogen, respectively.

In Fig. 6, the cavity resonance is close but not exactly aligned to the absorption line center. By applying a small DC voltage (~1.5 V in our experiment) to the PZT to change the cavity length, the cavity resonance near 1532.83 nm can be aligned precisely to the center of the P(13) line. The PT phase modulation is thus maximized. Fig. 7(a) shows the second harmonic signal output when pump laser is scanned across the resonance of the cavity close to the center of P(13) line and filled with 100 ppm acetylene. Fig. 7(b) shows the second harmonic output when the gas cell is filled with nitrogen. The peak values of the second harmonic signal in Figs. 7(a) and 7(b) are 52.0 μV and 4.3 μV, respectively, giving a PT signal due to acetylene absorption of ~47.7 μV. The second harmonic output signal from the lock-in when the pump is tuned to away from cavity resonances is regarded as noise and is shown in Fig.7(c). The noise over ~6.5-min duration has a standard deviation (s.d.) of 0.06 μV, only slightly larger than that when the pump is off (~0.05 μV). This gives a signal-to-noise ratio (SNR) of 795, and the noise equivalent concentration (NEC) for SNR of unity is estimated to be 126 ppb for a detection bandwidth of 0.031 Hz.

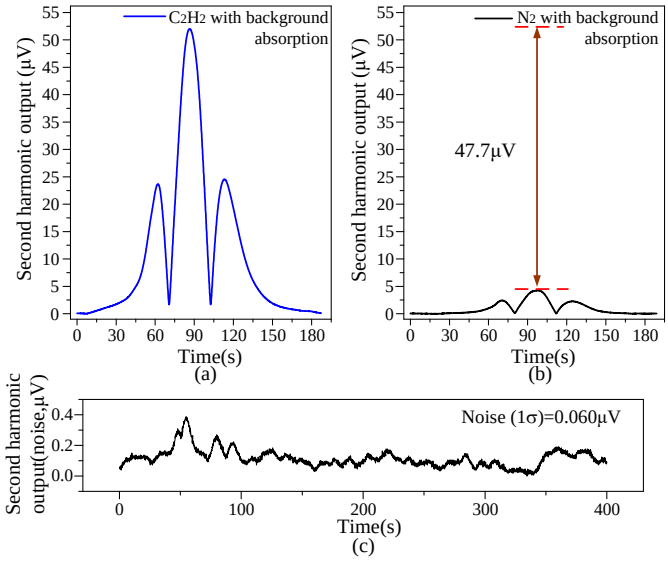

Fig. 7. Second harmonic signals when pump beam is scanned across a cavity resonance (Resonance A) near the center of the P(13) line of acetylene when the gas cell is filled with (a) 100 ppm acetylene and (b) pure nitrogen. (c) Second harmonic signal when the pump wavelength is away from Resonance A at 1532.9 nm.

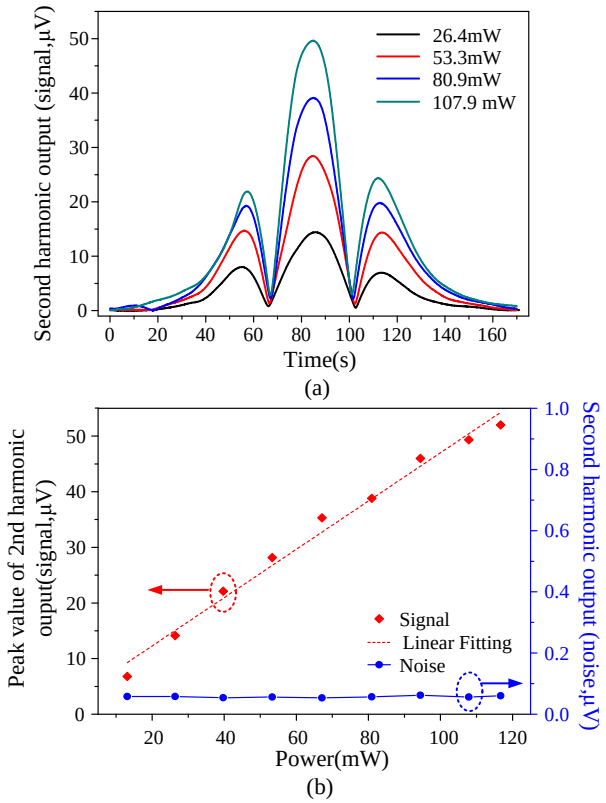

Fig. 8. (a) Second harmonic signals for four different pump power levels measured at the output of the 90:10 coupler. (b) The peak values of second harmonic signal (red squares) and the s.d. of the noise (blue circles) for increasing pump power level.

Fig. 8(a) shows the second harmonic output signal from the lock-in for different four pump power levels measured at the output of 90:10 coupler in Fig. 5 (a), when the pump wavelength was scanned across a cavity resonance aligned to the center of the P(13) line. The peak value of second harmonic signal and the s. d. of the noise as functions of pump power are shown in Fig. 8 (b). The second harmonic signal increases linearly with increasing pump power, while the noise level keeps more or less constant, indicating that the SNR may be further improved by increasing the pump power level.

V. Discussion

As mentioned in Section II, the phase detection is most sensitive when the probe wavelength is set to the maximum slope point of a cavity resonance, indicted as point 5 in Fig. 2. With the setup in Fig. 5, we experimentally evaluated the second harmonic output signal and the noise level for the 5 different operating points indicated in Fig. 2. The operating point was determined according to the DC output voltage, which was displayed in the oscilloscope as illustrated in Fig. 5 (a).

Fig. 9(a) shows the second harmonic output signal from the lock-in for the five different operating points shown in Fig. 2. The peak values of the second harmonic signal at Point 5 and Point 2 are 52.0 μV and 2.5 μV, respectively, showing ~20 times enhancement by operating at the maximum slope point of the resonance. The peak values of second harmonic output signal and the s. d. of the noise for the five operating points are shown in Fig. 9(b). The black squares show the peak values of the second harmonic signals and blue circles the s. d. of noise. The second harmonic output signal increases with the slope value of the cavity resonance while the noise level remained relatively flat, showing the signal to noise ratio is indeed enhanced when operating at point 5.

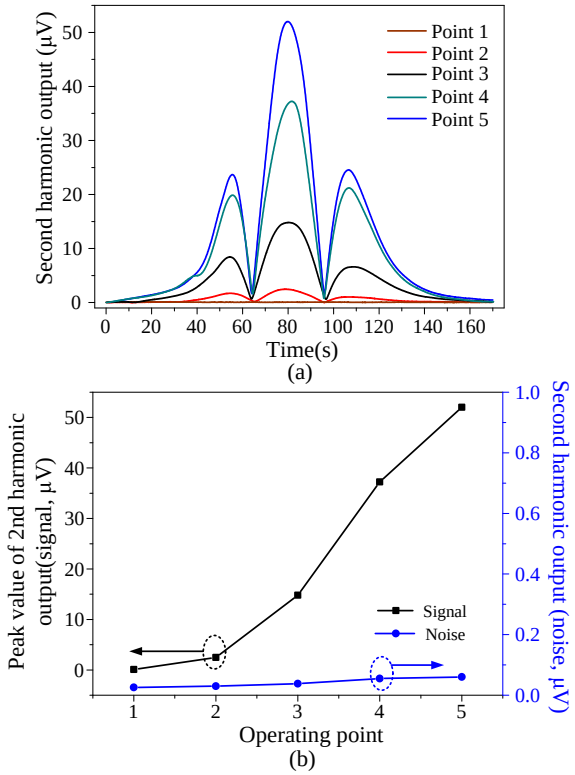

Fig. 9. (a) Second harmonic outputs (signal) when the probe is at five different operating points (1-5). (b) The peak values of second harmonic output signal

(black squares) and the s.d. of the noise (blue circles) at different operating points.

We have previously reported a PTI gas sensor with a low finesse HC-PBF F-P gas cell of 2 cm and achieved detection limit of 440 ppb using a 1s lock-in time constant [25]. This sensor was basically a single-path sensor a pump power of ~70 mW delivered into the gas cell, estimated by considering that the fusion splicing loss between SMF and HC-PBF is ~2 dB [21]. For comparison, the performance and the parameters of the present high-finesse and the previous low finesse F-P PTI sensors are summarized in Table I. The normalized noise equivalent absorption-coefficient (NNEA), in $cm^{-1}WHz^{-1/2}$, is improved by 3 to 4 times by using the high finesse F-P cavity.

TABLE I
PARAMETERS FOR HIGH FINESSE AND LOW FINESSE FABRY PEROT CAVITIES

Type of Fabry Perot	High finesse	Low finesse [25]
Acetylene absorption line (wavelength)	P(9):1532.83 nm	P(13):1530.37 nm
Peak absorption coefficient α for 1 ppm acetylene	1.05×10^{-6} cm^{-1}	1.165×10^{-6} cm^{-1}
Pump power into the cavity	0.0432 W	0.069 W
Detection bandwidth	0.031 Hz	0.094 Hz
Lower detection limit	126 ppb	440 ppb
NNEA	3.23×10^{-8} $cm^{-1}WHz^{-1/2}$	1.16×10^{-7} $cm^{-1}WHz^{-1/2}$

We were able to make HC-PBF F-P gas cells with cavity finesses up to 128 [14]. With such a cavity, the peak value of the slope is ~3 times higher than the present F-P cavity with finesse of 41. In addition, the use of a higher finesse cavity also further enhances the magnitude of PT phase modulation, which would further improve the detection limit.

VI. CONCLUSION

In conclusion, we presented a double-cavity-enhanced PTI gas sensor with a high finesse HC-PBF F-P cavity as the absorption cell. The high finesse gas cell is made by placing a length of HC-PBF between two the ends of two SMFs coated with reflective mirrors. With a 6.2-cm-long F-P with a finesse of 45 for pump beam and 41 for probe beam, we demonstrated acetylene detection down to 126 ppb, 1 to 2 orders of magnitude better than a direct absorption spectroscopic sensor with a similar high finesse HC-PBF cavity, and 3 to 4 times better than a low-finesse HC-PCF F-P PTI sensor. The use of a high finesse cavity simultaneously enhances the intra-cavity build-up for the pump intensity inside the HC-PBF and improves the phase detection sensitivity for the probe beam by a factor proportional to the cavity finesse. The performance of all fiber double-cavity-enhanced photothermal gas sensor may be further improved by using a cavity with a higher finesse.

REFERENCES

[1] C. C. Davis and S. J. Petuchowski, "Phase fluctuation optical heterodyne spectroscopy of gases," *Appl. Opt.* vol. 20, pp. 2539-2554, 1981.

[2] M. A. Owens, C. C. Davis, and R.R. Dickerson, "A photothermal interferometer for gas-phase ammonia detection," *Anal. Chem.* vol. 71, pp. 1391-1399, 1999.

[3] A. J. Campillo, S. J. Petuchowski, C. C. Davis, and H. B. Lin, "Fabry-Perot photothermal trace detection," *Appl. Phys. Lett.* vol. 41, pp. 327-329, 1982.

[4] S. E. Bialkowski, *Photothermal spectroscopy methods for chemical analysis* John Wiley & Sons, Inc., 1996.

[5] J. U. White, "Very long optical paths in air," *J. Opt. Soc. Am.* vol. 66, pp. 411-416, 1976.

[6] D. R. Herriott and H. J. Schulte, "Folded optical delay lines," *Appl. Opt.*, vol. 4, pp. 883-889, 1965.

[7] W. Jin, Y. Cao, F. Yang, and H. L. Ho, "Ultra-sensitive all-fibre photothermal spectroscopy with large dynamic range," *Nat. Commun.* vol. 6, pp. 6767, 2015.

[8] P. Russell, "Photonic Crystal Fibres," *Science* vol. 299, pp. 358-362, 2003.

[9] F. Yang, W. Jin, Y. Cao, H. L. Ho, and Y. Wang, "Towards high sensitivity gas detection with hollow-core photonic bandgap fibers," *Opt. Express* vol. 22, pp. 24894-24907, 2014.

[10] Y. L. Hoo, W. Jin, C. Shi, H. L. Ho, D. N. Wang, and S. C. Ruan, "Design and modeling of a photonic crystal fiber gas sensor," *Appl. Opt.*, vol. 42, pp. 3509-3515, 2003.

[11] C. Hensley, D. H. Broaddus, C. B. Schaffer, and A. L. Gaeta, "Photonic band-gap fiber gas cell fabricated using femtosecond micromachining," *Opt. Express*, vol. 15, pp. 6690-6695, 2007.

[12] A. van Brakel, C. Grivas, M. N. Petrovich, and D. J. Richardson, "Micro-channels machined in microstructured optical fibers by femtosecond laser," *Opt. Express*, vol. 15, pp. 8731-8736, 2007.

[13] Y. Hoo, S. Liu, H. L. Ho, and W. Jin, "Fast response microstructured optical fiber methane sensor with multiple side-openings," *IEEE Photonics Technol. Lett*, vol. 22, pp. 296-298, 2010.

[14] Y. Tan, W. Jin, F. Yang, Y. Qi, C. Zhang, Y. Lin, and H. L. Ho, "Hollow-core fiber-based high finesse resonating cavity for high sensitivity gas detection," *J. of Lightwave Technol.* Vol. 35, pp. 2887-2893, 2017.

[15] R. Van Zee and J. P. Looney, *Cavity-enhanced spectroscopies* vol. 40: Academic Press, 2003.

[16] L.-S. Ma, J. Ye, P. Dubé, and J. L. Hall, "Ultrasensitive frequency-modulation spectroscopy enhanced by a high-finesse optical cavity: theory and application to overtone transitions of C_2H_2 and C_2HD," *JOSA B*, vol. 16, pp. 2255-2268, 1999.

[17] A. Foltynowicz, *Fiber-laser-Based Noise-Immune Cavity-Enhanced Optical Heterodyne Molecular Spectrometry*, Doctoral Thesis, Umeå University, Sweden 2009.

[18] Y. Lin, F. Liu, X. He, W. Jin, M. Zhang, F. Yang, H. L. Ho, Y. Tan, and L. Gu, "Distributed gas sensing with optical fibre photothermal interferometry," *Opt. Express* vol.25, pp.31568-31585, 2017.

[19] Y. Lin, W. Jin, F. Yang, Y. Tan, and H. L. Ho, "Performance optimization of hollow-core fiber photothermal gas sensors," *Opt. Lett.* vol. 42, pp. 4712-4715, 2017.

[20] Y. Lin, W. Jin, F. Yang, J. Ma, C. Wang, H. L. Ho, and Y. Liu, "Pulsed photothermal interferometry for spectroscopic gas detection with hollow-core optical fibre," *Scientific reports* vol. 6, pp. 39410, 2016.

[21] L. Xiao, M. S. Demokan, W. Jin, Y. Wang, and C. L. Zhao, "Fusion Splicing Photonic Crystal Fibers and Conventional Single-Mode Fibers: Microhole Collapse Effect," *J. of Lightwave Technol.* Vol. 25, pp. 3563-3574, 2007.

[22] G. Gagliardi and H.-P. Loock, *Cavity-Enhanced Spectroscopy and Sensing*: Springer, 2014.

[23] L. S. Rothman, D. Jacquemart, A. Barbe, D. C. Benner, M. Birk, L. Brown, M. Carleer, C. Chackerian, Jr, K. Chance, L. Coudert, V. Dana, V. Devi, J. Flaud, R. Gamache, A. Goldman, J. Hartmann, K. Jucks, A. Maki, J. Mandin, S. Massie, J. Orphal, A. Perrin, C. Rinsland, M. Simth, J. Tennyson, R. Tolchenov, R. Toth, J. Auwera, P. Varanasi, and G. Wagner, "The HITRAN 2004 molecular spectroscopic database," *J. Quant. Spectrosc. Radiat. Transfer*, vol. 96, pp. 139-204, 2005.

[24] K. An, B. Sones, C. Fang-Yen, R. Dasari, and M. Feld, "Optical bistability induced by mirror absorption: measurement of absorption coefficients at the sub-ppm level," *Opt. Lett.* vol. 22(18), pp.1433-1435, 1997.

[25] F. Yang, Y. Tan, W. Jin, Y. Lin, Y. Qi, and H. L. Ho, “Hollow-core fiber Fabry–Perot photothermal gas sensor,” *Opt. Lett*. vol. 41(13), pp. 3025-3028, 2016.